Supplementary Material

Wireless "Janus" soft gripper with multiple tactile sensors

Lei Han,[a] Rui Wang,[a] Yupeng Dong,[a] Xun Zhang,[a] Chenggen Wu [a] and Xiaoguang Zhao [b]

[a] Key laboratory of MEMS of the Ministry of Education, Southeast University, Nanjing, 210096, China.
[b] Department of Precision Instruments, Tsinghua University, Beijing, 100084, China.

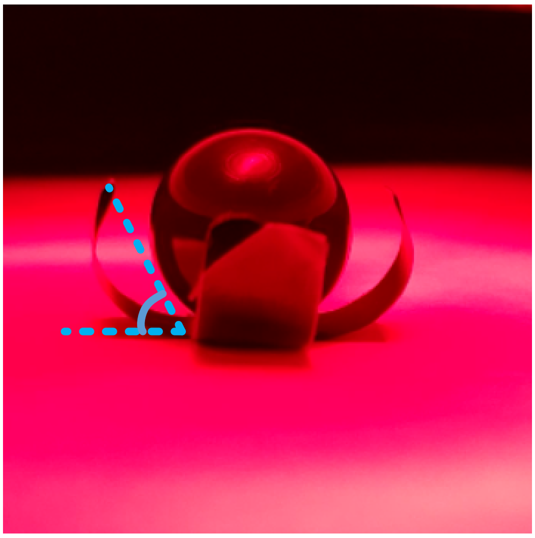

Fig.S1 Definition of the bending angle.

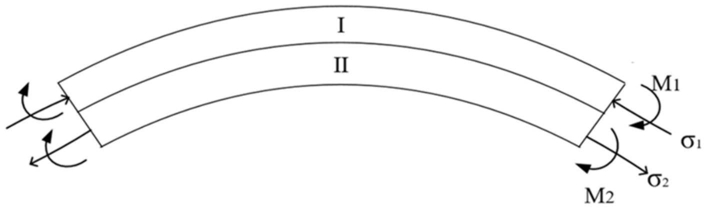

Fig. S2 Curvature of the bilayer film.

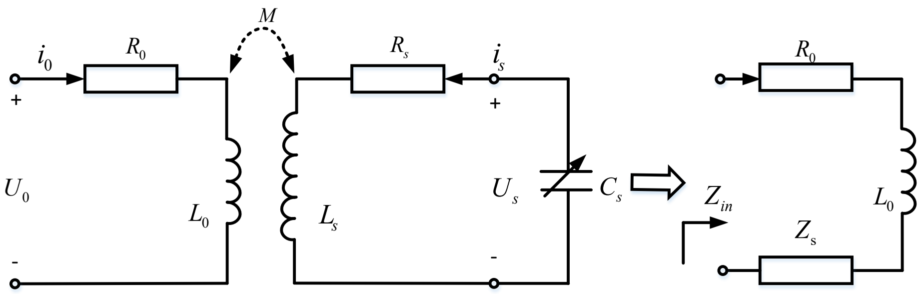

Fig. S3 Schematic of RLC circuit

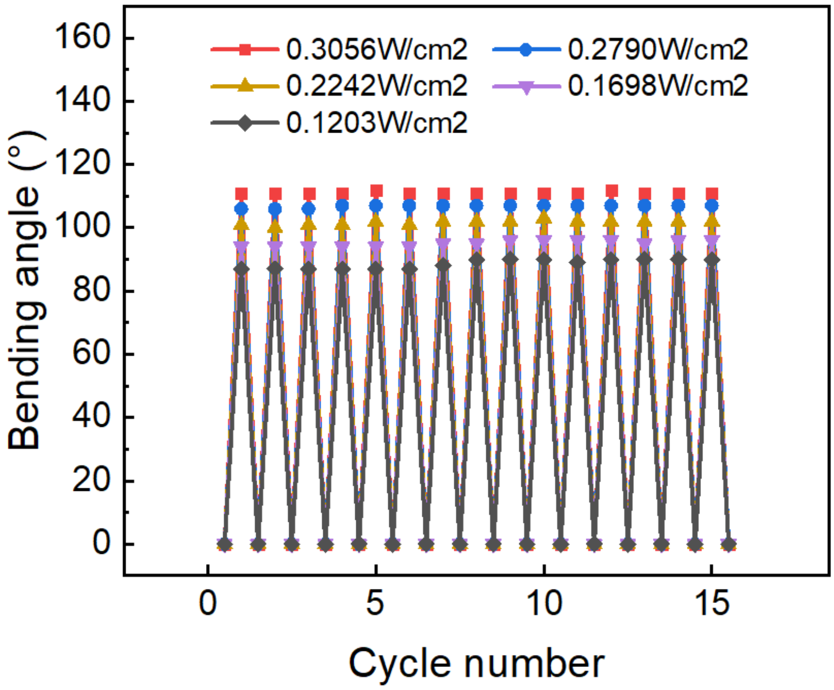

Fig.S4 Repeatability of the gripper movement.

Note S1

As shown in Fig. S2, σ and M represent internal stress and bending moment. The subscripts *1* and *2* represent each layer of film. A pair of forces equal in size and opposite in direction is generated between two layers, due to the difference in CTE. According to the static moment equilibrium

$$\frac{\sigma_1 t_1 + \sigma_2 t_2}{2} = M_1 + M_2 \tag{S1}$$

At the double-layer interface, the longitudinal strains are equal, so the curvature can be expressed as

$$Curvature = \frac{(\alpha_1 - \alpha_2)\Delta T}{\frac{t_1 + t_2}{2} + \frac{E_1 w_1 t_1^3 + E_2 w_2 t_2^3}{6(t_1 + t_2)}\left(\frac{1}{E_1 w_1 t_1} + \frac{1}{E_2 w_2 t_2}\right)} \tag{S2}$$

in which t, w, ΔT, a, and E are the thickness, width, temperature variation, CTE and Young's modulus respectively.

Note S2

The value of capacitance can be expressed simply as follows

$$C = \frac{\varepsilon_0 \varepsilon_r A}{D} \tag{S3}$$

where A and D are the distance and area of the capacitance plate. ε_0 is vacuum permittivity and ε_r is the relative permittivity of medium.

The perturbation from pressure and material changes causes the change in capacitance to be

$$\Delta C = \frac{A\varepsilon_0}{D}\Delta\varepsilon_r - \frac{A\varepsilon_0 \varepsilon_r}{D^2}\Delta D \tag{S4}$$

Note S3

According to Fig. S3, the quality factor Q and the resonant frequency f_s of the circuit are as follows.

$$Q = \frac{1}{R_s}\sqrt{\frac{L_s}{C_s}} \tag{S5}$$

$$f_s = \frac{1}{2\pi\sqrt{L_s C_s}} \tag{S6}$$

The input impedance Z_{in} at the port can be expressed as

$$Z_{in} = R_0 + j2\pi f L_0 \left(1 + \frac{k^2 \left(\frac{f}{f_s}\right)^2}{1 + j\frac{1}{Q}\frac{f}{f_s} - \left(\frac{f}{f_s}\right)^2} \right) \tag{S7}$$

The measured reflection coefficient S_{11} of the port is defined as

$$S_{11} = \frac{Z_{in} - Z_0}{Z_{in} + Z_0} \tag{S8}$$

which is equivalent to the impedance at the port, reflecting the change in resonant frequency.

Note S4

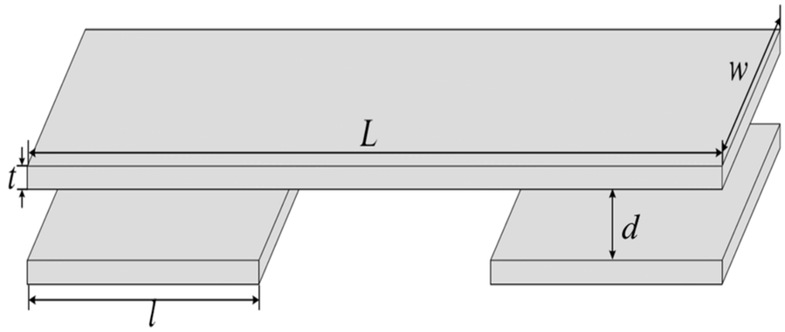

Fig. S5 Schematic diagram of pressure sensor electrodes.

As shown in Fig.S5, the three electrodes of the pressure sensor form two series capacitors to obtain pressure change. The width w and thickness t of each electrode are 3.5mm and 0.1mm. The length of the upper electrode L and the lower electrode l are 5mm and 2mm, respectively. d is the thickness of GO foam dielectric layer, which is 4mm.

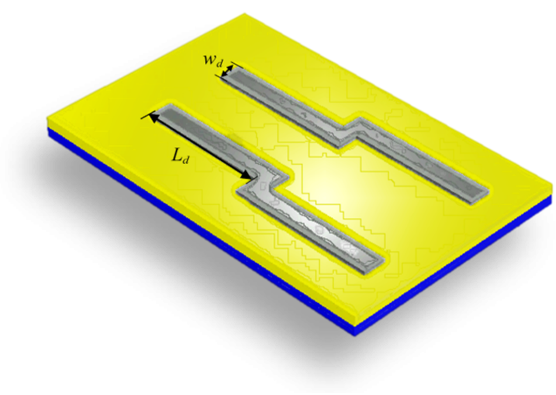

Fig. S6 Schematic diagram of material sensor electrodes.

As shown in Fig.S6, the interdigital electrodes of the pressure sensor consist of one group of interdigital structure. The width w_d and length L_d of each electrode are 1mm and 4mm. The thickness of electrodes is 0.1mm and the gap between two fingers is 2mm. Based on this initial parameter, an initial capacitance is obtained, which varies with the test material.

Note S5

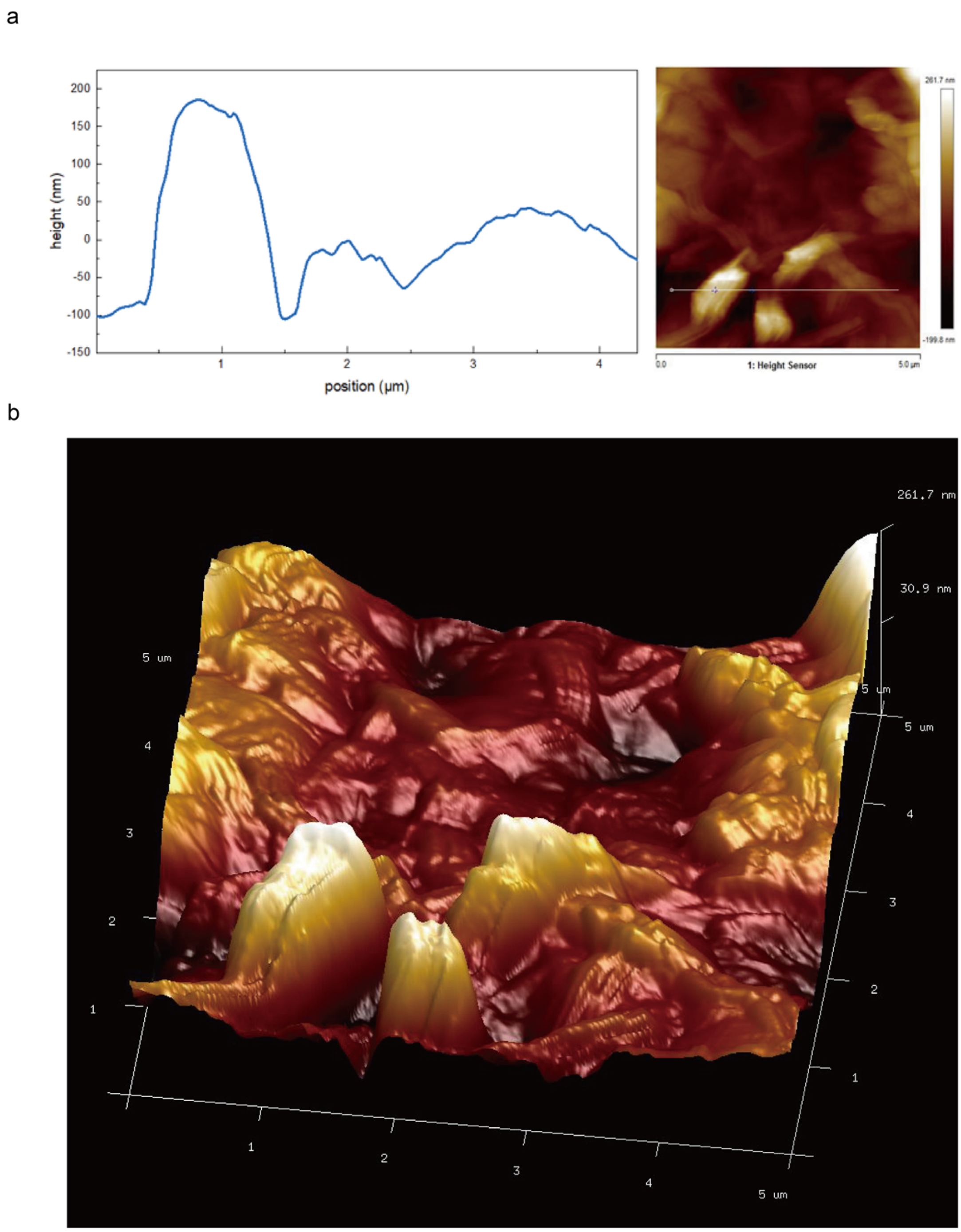

Fig. S7 AFM image of GO film. a. Height profile and 2D image; b. 5μm×5μm 3D image.

The AFM results shown in Fig.S7 show the maximum height drop is 288nm, which is negligible thickness compared to GO film. As the substrate layer of capacitors, GO film provides the initial dielectric constant for the fork finger capacitance. Here, ε is the equivalent dielectric constant, V is the percentage of volume, and the subscript denotes the corresponding component. According to the Lichtenecker formula (Eq. S9), the total dielectric constant depends on the component dielectric constants and the volume ratio they occupy. Since the gap due to roughness is negligible relative to thickness, it hardly affects the volume proportion of each component, which has no impact on sensing performance.

$$\ln\varepsilon = V_1 \ln\varepsilon_1 + V_2 \ln\varepsilon_2 \tag{S9}$$

Note S6

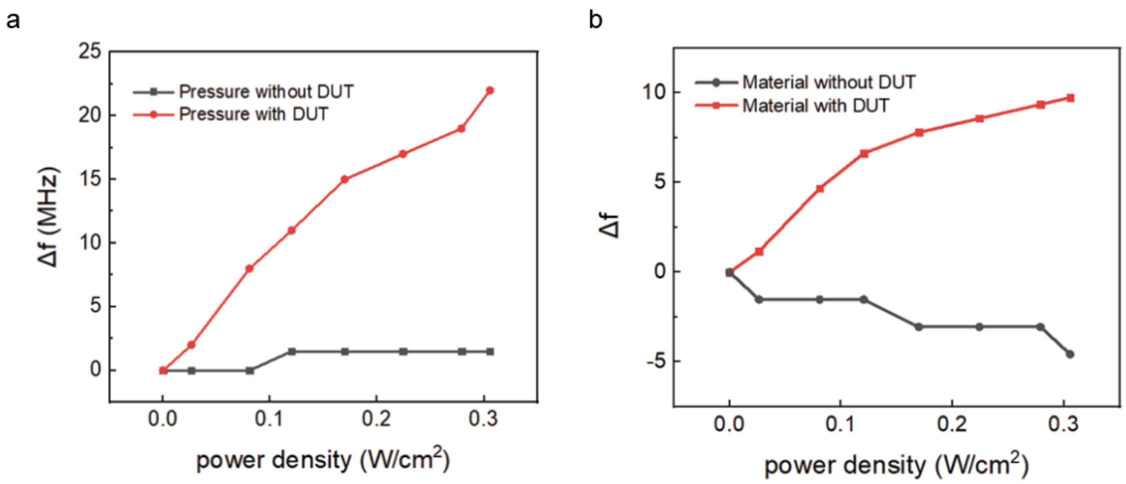

Fig. S8 Frequency shift with and without DUT. a. Pressure sensor; b. Material sensor.

As shown in Fig.S8a, the frequency shifts of pressure sensor without DUT are less than 2MHz under each power density, which is ignorable compared to that with DUT, which indicates that the performance of pressure sensor is not affected by movement.

The frequency shifts of material sensor without DUT exhibits a small shift in the reverse direction in Fig.S8b. Referring to Fig.5a, the reverse frequency shift means resonant frequency becomes higher. This is due to the dehydration of dielectric layer GO film at high temperatures resulting in smaller capacitance. Therefore, the resonant frequency increases and exhibits the opposite shift from that with DUT. This may be the reason why the shift with DUT does not behave linearly at high power density.

Because the reverse frequency shift of material sensor without DUT is relatively small compared to that with DUT, it does not affect the sensing of the material.

Note S7

Although there have been many studies on tactile sensors, we have found that these studies do not apply to a fully soft gripper. And wired sensing information transmission mode will also greatly limit the applicability. Hence, we compared this with previous sensors on the following aspects: the type of sensor, whether the sensor can be integrated into the soft grippers, and whether the sensing information can be wirelessly transmitted. These are shown in Table S3.

Note S8

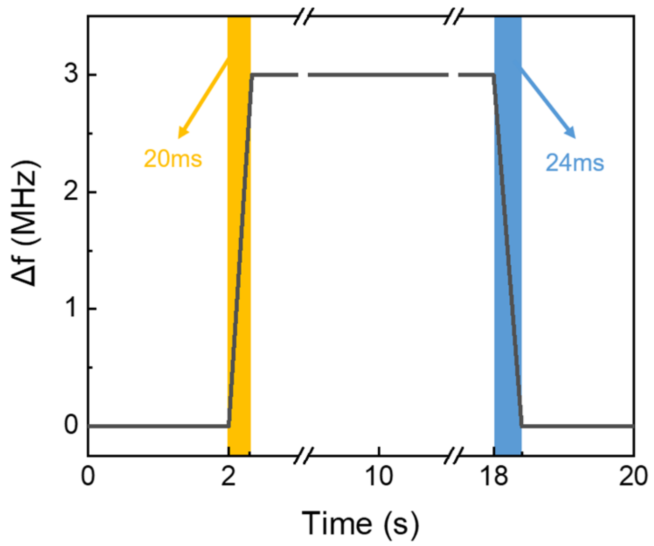

Fig. S9 Response of pressure sensor over a 20-second period.

To clarify the sensitivity of GO foam, we recorded the sensor response over a 20-second period. An external force of 28.5mN to squeeze the GO foam is applied after 2 seconds and is withdrawn after 18 seconds. The results are shown in the figure above. Without the external force, the frequency is fixed at the initial value at first. When the external force continuously squeezes the GO foam, a stable offset generates on the frequency. The time required to produce a stable offset is about 20ms. After the withdrawal of the external force, the frequency is back to the initial value in 24ms of recovery time.

Table S1 Dimensions of balls of different materials

	plastic	grass	wood	metal
Diameter (mm)	12、14、15、16	14、16	12、14、15、16	12、13、14、15、16

Table S2 Relative permittivity of different materials

	plastic	grass	wood	metal
Relative permittivity	2.3	3.5	4.3	conductive

Table S3 Comparation of this work with previous tactile sensors.

	Sensor type	Soft grippers applicability	Wireless
[1]	Pressure	No	Yes
[2]	Strain	Yes	No
[3]	Temperature Pressure	Yes	No
[4]	Temperature Pressure	Yes	No
[5]	Tactile	Yes	No
[6]	Temperature Pressure	Yes	No
[7]	Temperature Pressure Humidity	No	Yes
this work	Pressure Material	Yes	Yes

1. C. Wang, D. Hwang, Z. B. Yu, K. Takei, J. Park, T. Chen, B. W. Ma and A. Javey, *Nature Materials*, 2013, **12**, 899-904.
2. C. Y. Yan, J. X. Wang, W. B. Kang, M. Q. Cui, X. Wang, C. Y. Foo, K. J. Chee and P. S. Lee, Advanced Materials, 2014, **26**, 2022-2027.
3. M. Jung, K. Kim, B. Kim, H. Cheong, K. Shin, O.-S. Kwon, J.-J. Park and S. Jeon, Acs Applied Materials & Interfaces, 2017, **9**, 26974-26982.
4. C. Y. Wang, K. L. Xia, M. C. Zhang, M. Q. Jian and Y. Y. Zhang, Acs Applied Materials & Interfaces, 2017, **9**, 39484-39492.
5. S. Chun, I. Hwang, W. Son, J. H. Chang and W. Park, Nanoscale, 2018, **10**, 10545-10553.
6. T. Tran Quang, S. Ramasundaram, B.-U. Hwang and N.-E. Lee, Advanced Materials, 2016, **28**, 502.
7. Q. Tan, W. Lv, Y. Ji, R. Song, F. Lu, H. Dong, W. Zhang and J. Xiong, Sensors and Actuators B-Chemical, 2018, **270**, 433-442.

Supplementary Movie

Four types of balls are tested to demonstrate the gripper system.